Journal of Engineering Science and Technology
Vol. 12, No. 10 (2017) 2567 - 2584

DEFECTED CONCRETE POST DETECTION THROUGH ANTENNA ARRAY COUPLING EFFECT

TAMER G. ABOUELNAGA*, KAMEL S. SULTAN

Microstrip Circuits Department, Electronics Research Institute, National Research Center Buildings, Eltahrir St., Eldoki, Giza, Egypt
*Corresponding Author: tamer@eri.sci.eg

Abstract

In this paper, a proposed defected concrete post detection system is introduced. The proposed system consists of two compact microstrip broad side antenna arrays resonating at 1 GHz with dimensions of 45 cm by 13.2 cm for each antenna array and a weight of 800 gm for both antenna arrays. Also a portable vector network analyser is used for scattering parameters measurement purpose. For size comparison purpose, a conventional microstrip antenna array is designed and compared with the proposed one at the same resonant frequency. A size reduction of 23.4 % is obtained. The proposed antenna array directivity of 10.5 dBi and 3 dB beam width of 30.7 are obtained which are suitable for the concrete post defect detection. The detection principle is relied on the coupling between the two antenna array elements. Three cases are considered for simulation and measurement, air, good concrete block and defected concrete block. A 10 dB difference in coupling was obtained between the presence and the absence of the defect in the concrete block. A proposed measurement system is introduced. Good agreement is obtained between measured and simulated results. The proposed defected concrete post detection system is noticed to be light weight, simple, cheap and has a reasonable accuracy level.

Keywords: Microstrip antenna, Broad side antenna array, Compact antenna array, S-parameters, Non-destructive test.

1. Introduction

After the concrete has hardened, it is often necessary to test concrete structures to determine whether the structure is suitable for its designed use or not. The tests available for testing concrete range from the completely non-destructive, where there is no damage to the concrete, through those where the concrete surface is slightly damaged, to partially destructive tests, such as core tests and pull out and

Nomenclatures

A_{n-1}	Nth-1 weighted factor
G_1	Slot self-input conductance
G_{12}	Slot mutual conductance
h	Microstrip antenna substrate thickness
k	Wave number
k_o	Free space wave number
L	Microstrip antenna length
N	Integer number
R_{in}	Microstrip antenna input impedance
w	Microstrip antenna width
Zo	Characteristic impedance

Greek Symbols

β	Excitation phase for each element
ε_r	Relative dielectric constant
ε_{reff}	Effective relative dielectric constant
λ	Wave length
λ_o	Free space wave length
ϕ	Denotes the direction angle of the far-field
ψ	Array factor phase

Abbreviations

AF	Array Factor
CST	Computer Simulation Technology
EF	Element Factor

pull off tests, where the surface has to be repaired after the test. Non-destructive testing (NDT) can be applied to both old and new structures [1].

A radar system is one of the most important systems which could be used in non-destructive tests. The detection and penetration capabilities of radar system can be optimized by adjusting its center frequency and bandwidth. The electromagnetic properties of concrete are related to the physical condition of concrete such as moisture level, composition of concrete mix as well as the frequency of incoming electromagnetic waves from radar. In performing radar measurements, other factors such as polarization and incident angle of the electromagnetic waves, power and dynamic range of radar, and measurement distance also affect results [2].

The target detection principle may be depended on investigating the coupling signal between two antennas (single element or array) or investigating the reflected signal using one antenna. Many applications such as buried object detection, tunnels detection, landmines detection and tumors detection had used one of these principles of detection.

The detection process of the buried targets based on the coupling between using two parallel microstrip antennas was proposed by Zainud-Deen et al.[3]. The antennas were placed on same ground plane with defected ground structure

between them that had the advantage of a low mutual coupling compared with the classic one. The Finite-Difference Time-Domain (FDTD) was used to simulate the sensor for landmines detection.

Lorenzo et al. [4] introduced a tunnel detection method based on the scattered wave from the target. Diffraction tomography and inverse-scattering principles were applied and inversion methods to reconstruct images were proposed. When antennas were located belowground, there are three different modes of propagation. These modes are direct, reflected, and lateral waves. They are existed between transmitter and scatterer, and between scatterer and receiver. Using vertical dipoles, vertical ferrite-loaded coils, or gradiometer antennas, the effect of lateral wave may be reduced.

Cepni et al. [5] described a single antenna time-reversal based detection scheme that could be used to enhance the performance of a radar system in a multipath rich scattering environment. The experimental results showed that depending on the amount of clutter in the medium, the performance of a radar detection scheme could be improved up to 4.8 dB using time-reversal methods with a single antenna.

Chen et al. [6] presented an ultrawide-bandwidth dielectric-rod antenna for shallow targets detection, such as antipersonnel (AP) mines. The antenna near-field radiation properties were investigated. Both measurement and numerical simulation results were presented for the detection of buried AP mines using a prototype dielectric-rod antenna operated at a frequency range from 1 to 6 GHz.

Kim et al. [7] presented a target-detection with electronically-steerable array (ESA) antenna. A 2×2 ESA antenna was designed, fabricated and tested for two-dimensional beam steering. Unlike standard horn antennas that exhibit no electronic steering, the 2×2 ESA was able to identify a target location by steering the beam angle.

Simi et al. [8] developed Subsurface Tomographic Radar Equipment (STREAM) GPR system. Large and high dense multi-frequency antenna arrays had been developed to be mounted on a vehicle-towed trolley to assure a quick and correct data collection. Thanks to its dual polarized dense array STEAM assured high performance in terms of data quality (especially for tomographic output) and accordingly high detection capability.

Same concept has been used in the medical field especially in the early breast cancer detection. An ultra-wideband (UWB) microwave system for breast cancer detection had been presented by Klemm et al. [9]. The system was based on a novel hemispherical real-aperture antenna array, which was employed in a multi-static radar-based detection system. The array consisted of 16 UWB aperture-coupled stacked-patch antennas located on a section of a hemisphere. The radar system was designed to be used with realistic three-dimensional (3D) breast phantoms, which had been developed, as well as with real breast cancer patients during initial clinical trials. Experimental results were presented, demonstrating the successful detection of 4 and 6 mm diameter spherical tumors in the curved breast phantom.

Nilavalan et al. [10] presented a patch antenna which had been designed to radiate into human breast tissue. The antenna was shown by means of simulation and practical measurement to possess a wide input bandwidth, stable radiation patterns

and a good front-to-back ratio. Consideration was also given to its ability to radiate a pulse, and in this respect it was also found to be suitable for the cancer detection application. Table 1 shows a comparison among previous different microwave systems and the proposed one considering frequency, size and applications.

In this paper, the study is focused on the air gap detection in concrete posts through investigating the coupling factor between two antenna arrays in the presence of good concrete post and defected one. Both antenna arrays are designed to be resonated at 1 GHz and with 3 dB beam width of about 30.7 degree. The distance between the two antenna arrays is optimized for the defects detection best condition. So, our proposed system has to be calibrated first. The paper discuss conventional microstrip four elements broadside antenna array in its first section. Then, in second section, the proposed compact four elements antenna array is designed, simulated results are investigated. In third section of the paper, the proposed system setup is introduced and the measurement results are discussed. Finally the conclusion is presented.

Table 1. Comparison between proposed system and previous work.

Reference	Single antenna size (mm^2)	Substrate ($\varepsilon_r, h\ (mm)$)	Frequency (GHz)	(Application, Developed)
3	53.2×45.6	(10.2, 9.645)	0.790	Landmines detection, No
4	600×76	(3,76)	Bandwidth (2-6)	GPR, Yes
10	6.5×9	(10.2,4.61)	4.2	Breast cancer detection, Yes
Proposed	80×59	(4.5,1.5)	1	Defected concrete ,Yes

2. Broadside Antenna Array

An antenna array is a collection of two or more antennas working in concert to set up a unique radiation pattern for the electromagnetic environment at hand. A necessary characteristic of an array is the change of its radiation pattern in response to various excitations of its antenna elements. Unlike a single antenna whose radiation pattern is fixed, an antenna array's radiation pattern, called the array pattern, can be changed upon exciting its elements with different currents (both current magnitudes and current phases). This gives us a freedom to choose (or design) a certain desired array pattern from an array, without changing its physical dimensions. Furthermore, by manipulating the received signals from the individual antenna elements in different ways, we can achieve many signal processing functions such as spatial filtering, interference suppression, gain enhancement, target tracking, etc. Antenna arrays are becoming increasingly important in wireless communications [11-14]. In linear arrays, all elements are aligned along a straight line and generally have uniform element spacing as shown in Fig. 1. The minimum length linear array is the 2-element array. For N isotropic elements which are separated by an equal distance d and a phase reference at the first element n = 1, the radiated field at a large distance away for the array is given as

$$AF = \sum_{n=1}^{N} A_{n-1}\, e^{j(n-1)\psi} \quad (1)$$

where

$$\psi = kd\cos\varphi + \beta \tag{2}$$

where $k = (2\pi/\lambda)$ is the wave number, λ is the wavelength in free space, φ denotes the direction angle of the far-field which is measured from the horizontal axis and β is the excitation phase for each element. If the phase reference is chosen at the center of the array and the amplitudes are uniform and equal to unity, the radiated field can be written in normalized form as

$$AF_n = \frac{1}{n}\frac{(1-e^{jn\psi})}{(1-e^{j\psi})} = \frac{1}{n}\frac{sin(n\psi/2)}{sin(\psi/2)} \tag{3}$$

The element factor (EF) is the far field equation for single antenna element and the array factor (AF) is the pattern function associated with the array geometry. The distant field from an array of identical elements can always be broken down into the product of the element factor (EF) and the array factor (AF). The very fact that the antenna pattern can be multiplied by the array factor pattern demonstrates a property called pattern multiplication.

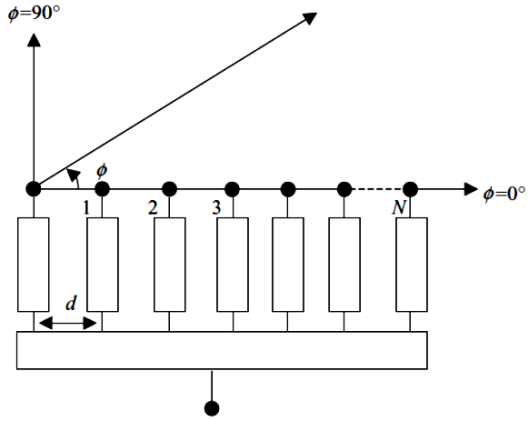

Fig. 1. Linear antenna array configuration.

We now consider broadside array because its suitability to the concrete posts air gap detection. In a broadside array of *N* isotropic point sources, the radiation pattern is perpendicular to the plane of the array and the amplitude and phase of the elements are equal. Thus, the phase term of Eq. (2) reduces to

$$\psi = kd\cos\varphi \tag{4}$$

The maximum value of the field occurs when $\psi = 0$, this occurs when $\varphi = (2m + 1)\pi/2$, where m is an integer value (i.e. m = 0, 1, 2 ...). Thus, the field is a maximum when $\varphi = \pi/2$ and $\varphi = 3\pi/2$. Matlab code has been built to predict the normalized field patterns for broadside arrays. Figure 2 shows the normalized field patterns for broadside arrays of eight elements with spacing $d = \lambda/2$ and $d = \lambda$, respectively. One can notice the appearance of the grating lobes at 180 and 0 degree when $d = \lambda$. Also the beam width becomes narrower with increasing the number of elements as shown in Fig. 3.

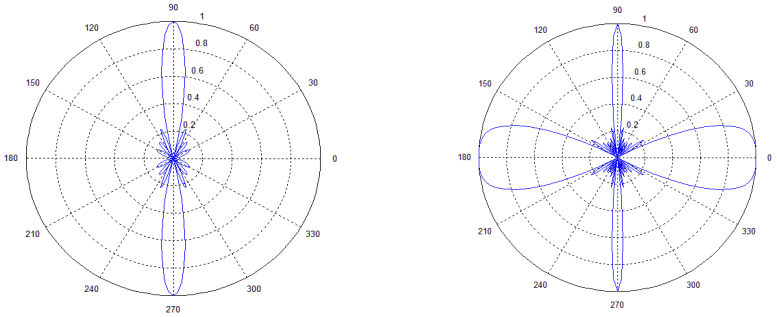

(a) **(b)**

Fig. 2. Broadside normalized array field patterns for an eight-element with (a) spacing $d = \lambda/2$ and (b) spacing $d = \lambda$.

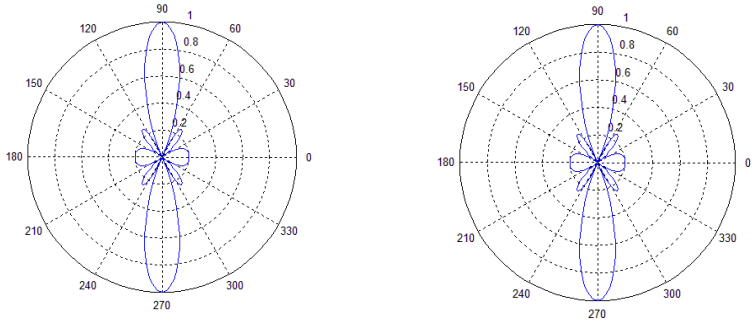

N=5 N=7

Fig. 3. Broadside normalized field patterns with spacing $d = \lambda/2$ and (a) N=5 and (b) N=7.

2.1. Conventional microstrip antenna array

Antenna array performance depends on element shape, spacing, excitation and the pattern of array elements. The array performance can be increased by increasing number of elements but size, cost and complexity should be considered [15]. In this section, four elements conventional microstrip antenna array are introduced. Firstly, conventional rectangular microstrip patch antenna is investigated and a design flowchart is developed. Secondly, this conventional microstrip antenna is used to develop a four elements antenna array and finally the obtained results are investigated.

2.1.1. Single antenna element

Conventional rectangular microstrip patch antenna, Fig. 4 is designed, [16]. Flowchart of antenna design steps is shown in Fig. 5. The procedure assumes that the specified information includes the dielectric constant of the substrate ϵ_r, the resonant frequency f_r, and the height of the substrate h are known.

Based on the flowchart, Fig. 5, a rectangular patch antenna operates at about 1 GHz is designed. The antenna is designed over FR4 material with $\epsilon_r = 4.5$, $tan\,\delta = 0.025$ and thickness $h = 1.5$ mm. The antenna width $W = 90$ mm and

antenna length $L = 68.5$ mm. The antenna input impedance and the feed line width w_o are calculated by [17] and [18], respectively. The inset distance y_o is calculated for input impedance, [17] of 50 Ω to be $y_o = 26$ mm and the feed line width w_o is calculated to be $W_o = 2.85$ mm. As shown in Fig. 6, the reflection coefficient of the antenna shows that good matching at 1.01 GHz is obtained. Bandwidth of about 10 MHz is obtained.

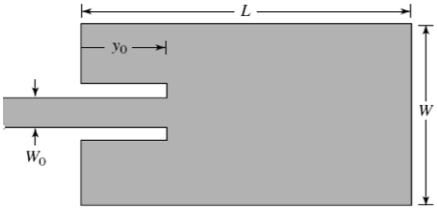

Fig. 4. Conventional rectangular microstrip antenna.

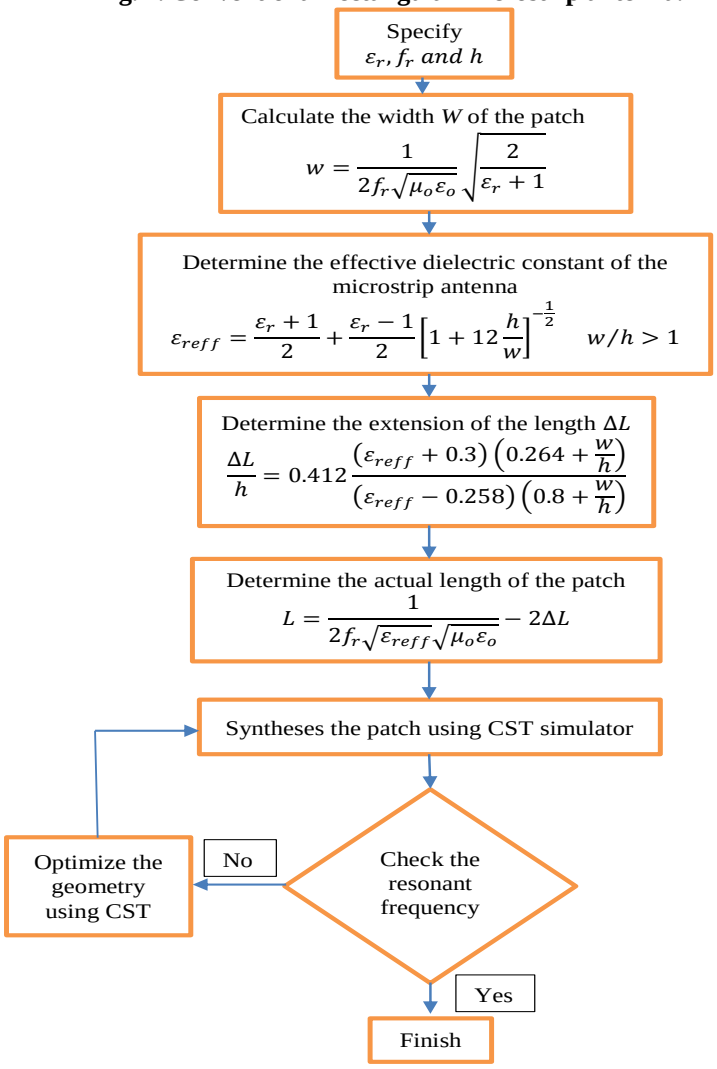

Fig. 5. Conventional rectangular microstrip antenna design flow chart.

Figure 7 shows the radiation pattern of the antenna, one noticed that the antenna is broadside radiator and the radiation in *x-y* plane is zero. Also, the directivity of the antenna is 5.6 dBi and the beam width is 100.6^{o} in the yz plane and 95.6^{o} in the xz plane. Both results are not good enough for concrete defects detection. So, an antenna array will be designed.

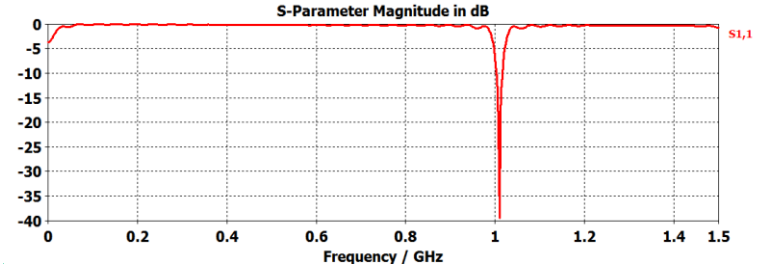

Fig. 6. Rectangular patch return loss.

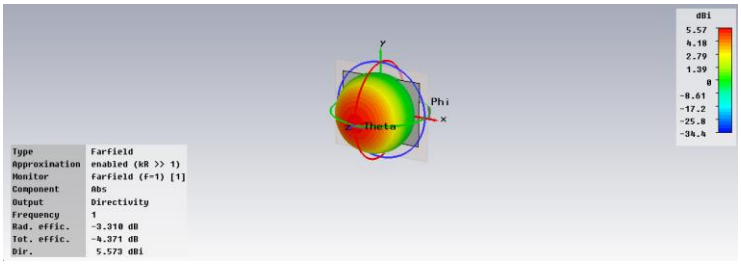

Fig. 7 (a). 3-D radiation pattern.

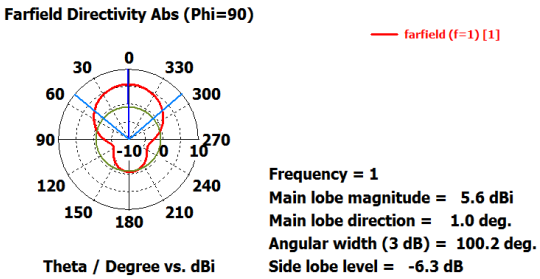

Fig. 7(b). YZ plane radiation pattern

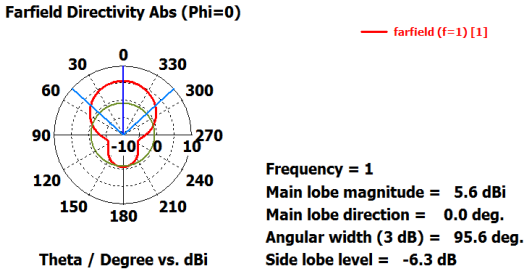

Fig. 7(c). XZ plane radiation pattern.

2.1.2. Four elements antenna array

The designed single patch antenna is used to design a 4×1 antenna array operates at 1 GHz. Figure 8 shows the geometry of the 4×1 antenna array designed to operate at 1 GHz with distance between elements equal $\lambda/2$ and feeding network based on $\lambda/4$ transformer, [18]. The reflection coefficient of the antenna array is shown in Fig. 9 and the radiation pattern of the proposed antenna array with high directivity equal to 10.6 dBi is shown in Fig. 10.

Figure 10 shows the radiation pattern of the proposed antenna in 3-D, XZ plane and YZ plane the radiation pattern is broadside and the directivity of the antenna at 1 GHz is 10.6 dBi. Half power beam width = 32.3^{o} which is very suitable to the concrete defects detection system.

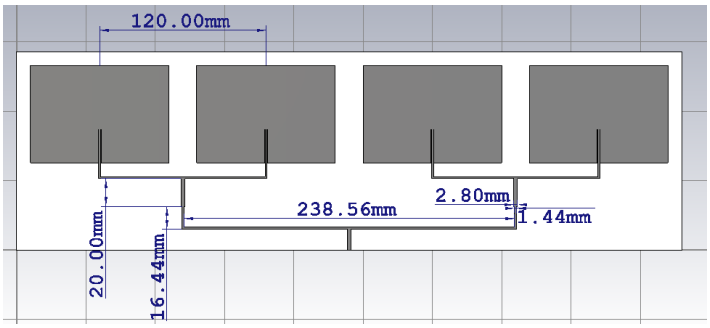

Fig. 8. Structure of antenna array.

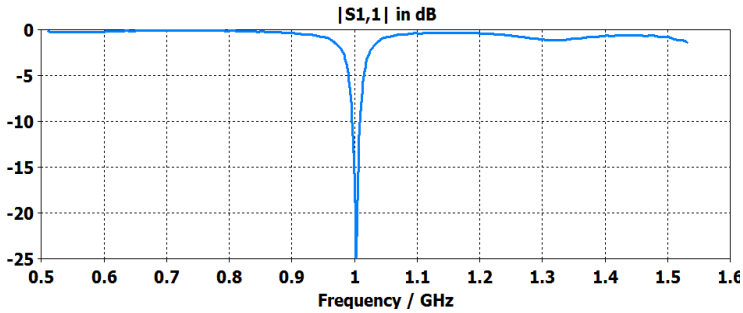

Fig. 9. Antenna array reflection coefficient.

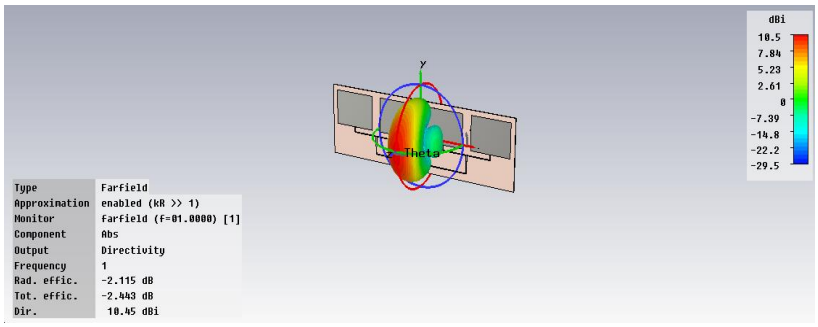

Fig. 10(a). Antenna array 3-D radiation Pattern.

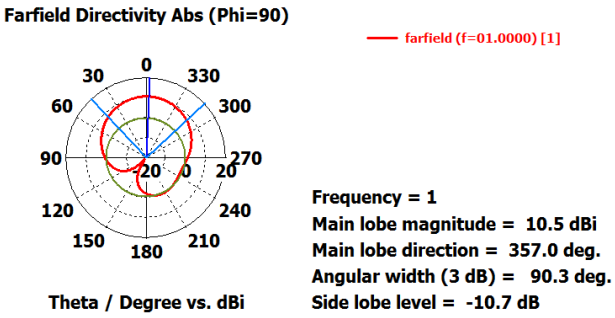

Fig. 10(b). YZ plane antenna array radiation pattern.

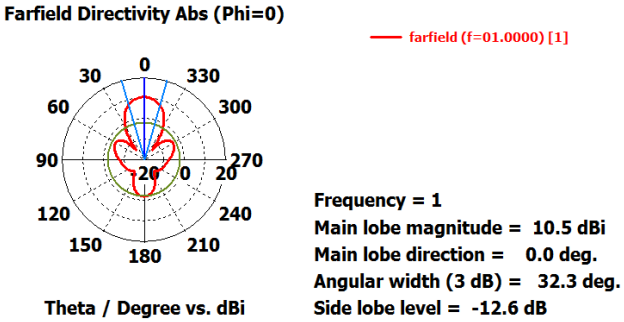

Fig. 10(c). XZ plane antenna array radiation pattern.

Table 2 shows a comparison between single and four elements antenna array parameters (main lobe width, directivity and side lobe level).

Table 2. Comparison between one element and four elements antenna.

	Parameter	One element	Four elements
XZ (phi=0)	**Main beam width**	95.3 deg.	32.3 deg.
	Directivity	5.6 dBi	10.5 dBi
YZ (phi=90)	**Main beam width**	100 deg.	90.3 deg.
	Directivity	5.6 dBi	10.5 dBi

2.2. Compact microstrip broadside antenna array

The main challenges of the microstrip antenna array are narrow bandwidth and size reduction. Many bandwidth enhancement methods had been used such as adding a straight slot parallel and near to the patch top side or using a defected ground structure DGS [20-21]. Miniaturization is also be achieved by using high dielectric substrate or using artificial ground structure called Reactive impedance surface (RIS) [22]. In this section, four elements compact microstrip antenna array are introduced. Firstly, compact slotted rectangular microstrip patch antenna is designed. Secondly, the developed slotted microstrip antenna is used to develop a four elements antenna array and finally the obtained results are investigated.

2.2.1. Single element

One of the most used antenna miniaturized techniques is to increase the electrical length of antenna which could be done by inserting slots in current path. Meandering forces the current to flow through a longer path, increasing the effective dimensions of the patch. The meandering can be achieved by inserting several narrow slits at the patch's non radiating edges. Figure 11 shows the geometry of compact antenna. The antenna with slot is operated at 0.83 GHz with the same dimensions of the previous antenna. The next step is to redesign the antenna to resonant at 1 GHz with optimized dimensions. All labelled dimensions for the proposed antenna is given in Table 3 for the same shape but with different dimensions. Hence, we note that the size reduction ratio (SRR) can be evaluated as follows:

Conventional antenna area (CAA) = 68.5×90 mm^2
Proposed compact antenna area (PCAA) = 59×80 mm^2

$$SRR = \frac{CAA - PCAA}{CAA} = \frac{6165-4720}{6165} = 23.4\ \% \quad (8)$$

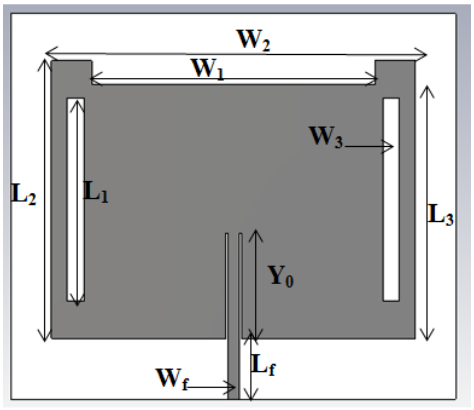

Fig. 11. Compact antenna geometry.

Table 3. Compact antenna dimensions.

Antenna Parameter	Proposed antenna with same dimensions as conventional one	Proposed antenna with optimized dimensions
f	0.83 GHz	1 GHz
L_1	50	46
L_2	68.5	59
L_3	62.5	55
L_f	15	15
W_1	70	70
W_2`	90	80
W_3	4	4
W_f	2.85	2.85
Y_0	26	22

2.2.2. Antenna array

The proposed compact antenna is used to design an array with four elements and $\lambda/4$ transformer feeding network, Fig. 12. One should mention that the microstrip antenna array gain can be enhanced by controlling the element space [23] but the side lobe level should be noticed. . The antenna array has been designed to operate at 1 GHz with a $\lambda/2$ separation between the elements. The reflection coefficient of the proposed antenna array is shown in Fig. 13 where a good matching is achieved at 1 GHz. The radiation pattern of the proposed antenna array is shown in Fig. 14 where a high directivity of 10.6 dBi.

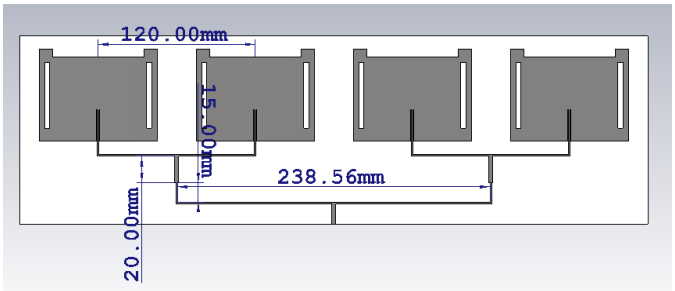

Fig. 12. Geometry of antenna array.

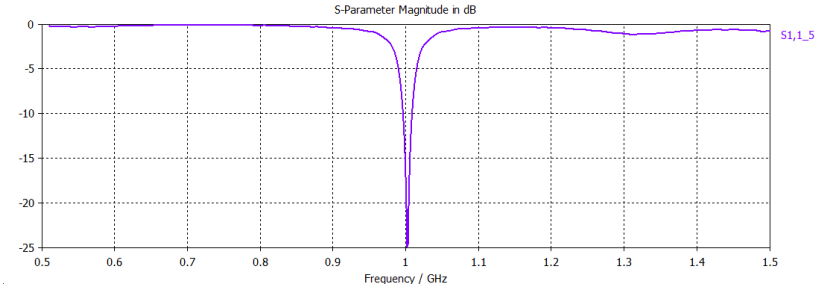

Fig. 13. Reflection coefficient of the proposed antenna array versus frequency.

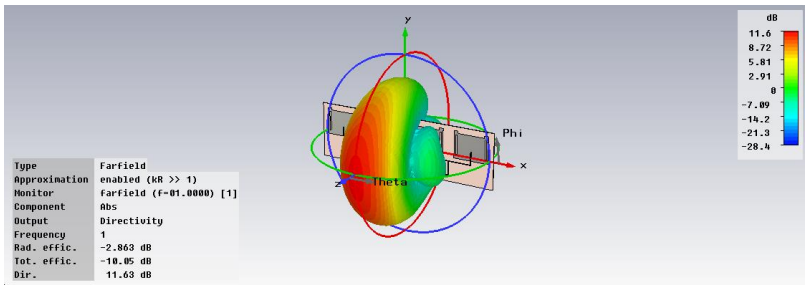

(a) 3-D radiation Pattern

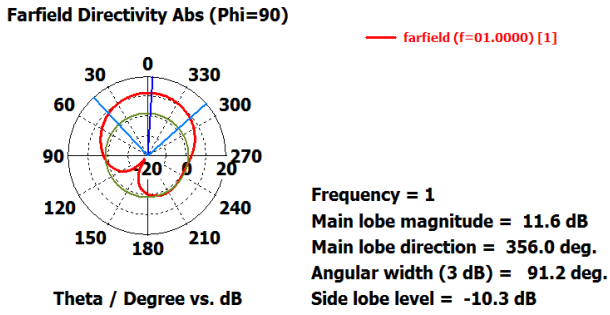

(b) YZ Plane

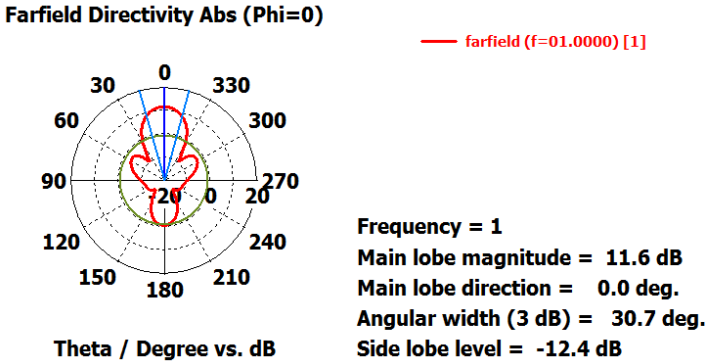

(c) XZ Plane

Fig. 14. Radiation pattern of the proposed compact antenna array.

3. Proposed System Setup, Simulation and Measurement

In this section, the proposed system setup is introduced, simulation results using CST software are obtained and simulation results are discussed. Finally the proposed system is fabricated, measured and both simulated and measured results are compared.

3.1. Simulation setup

Two identical antenna arrays are placed in free space at distance of 30 cm and the coupling factor is obtained in free space, with concrete and with defect concrete blocks as shown in Figs. 15 and 16. The dimensions of concrete block and spacing between antenna array and concrete are $L_1 = 50cm, L_2 = 50\ cm, L_4 = 10\ cm\ and\ L_3 = 10\ cm$. The one year old concrete dispersive material is given in CST simulator library as $\varepsilon_r = 5.5 + j0.11$. The distance between antenna array and the concrete block depends on the beam width of antenna array. We note that in air case, the coupling between two antennas is large compared with the case where the concrete block is placed between them. When the defected-concrete block is placed instead of the good one, the obtained coupling is an intermediate value between that value of air and

concrete block. At 1 GHz, a 10 dB difference is obtained between the coupling values of defected and good concrete block. This coupling difference value is detectable by any power sensor. The distance effect between antenna array and the concrete block is shown in Fig. 18. One can notice that, as the distance increases from 8 cm to 20 cm the coupling decreases. However, increasing the distance to 30 cm, the coupling increases again. That is because, the radiation pattern of both antenna arrays will no more concentrated on the concrete block only but considerable portion will be coupled through the air.

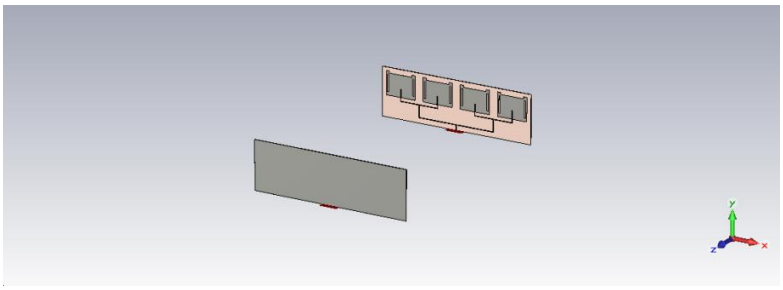

Fig. 15. Transmitted and received antenna in Free space.

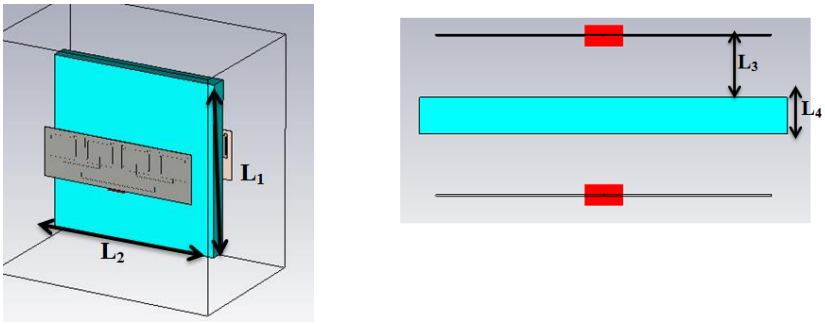

(a) **(b)**

Fig. 16. Transmitted and received antenna array with concrete.

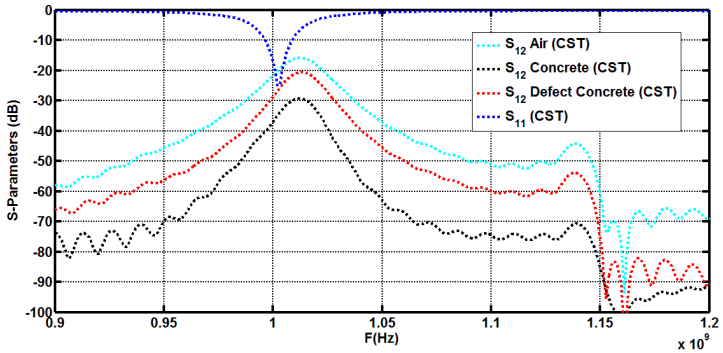

Fig. 17. S-parameters of the proposed system versus frequency for air, concrete and defected concrete.

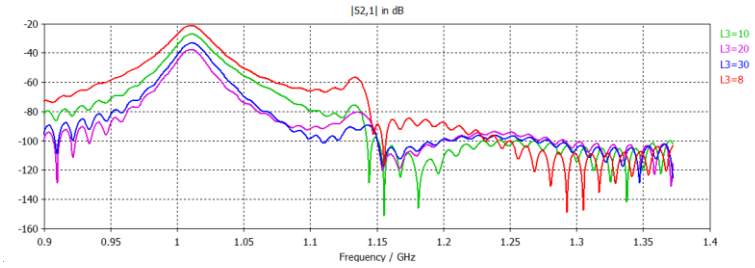

Fig. 18. S_{21} versus frequency as the distance between concrete block and antenna array is varied.

3.2. Measurement setup

The proposed antenna array is fabricated on FR4 material with thickness of 1.5 mm and dielectric loss of 0.025, Fig. 19. The reflection coefficient of the proposed antenna array is measured using vector network analyser which is shown in Fig. 20 where good agreement between the measured and the simulated results is noticed. The proposed measurement system is shown Fig. 21 where the concrete and the antenna arrays are fixed using a wood stand. A portable VNA is used for measurement purpose. As it was planned, the coupling coefficient has been measured in three different cases namely, air, good concrete and defected concrete blocks, Fig. 22. Good agreement between simulated and measured S parameters which is shown in Fig. 23 for the aforementioned three cases. A measured 10 dB coupling difference at 1 GHz is noticed between the presence and the absence of the defect in a concrete block which indicates the simplicity of the defect detection in the proposed system.

Fig. 19. Fabricated proposed antenna array photo.

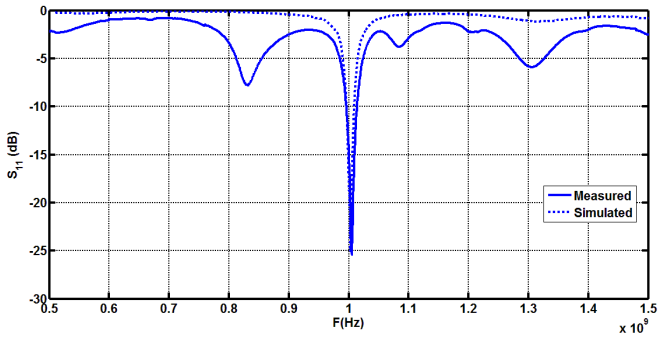

Fig. 20. Measured and simulated reflection coefficient versus frequency.

Fig. 21. Proposed measurement system using potable VNA.

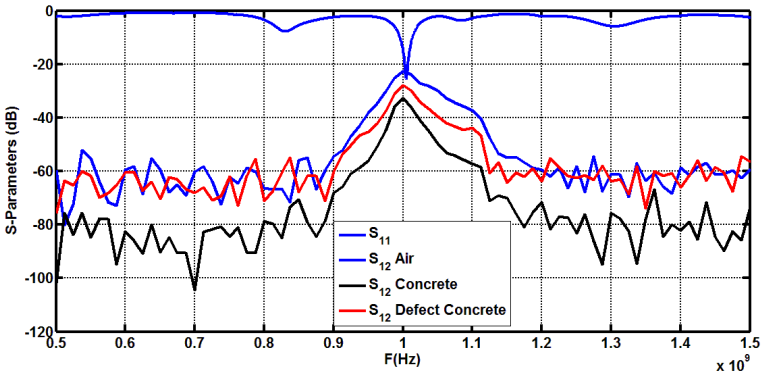

Fig. 22. Measured S parameters versus frequency of the proposed system.

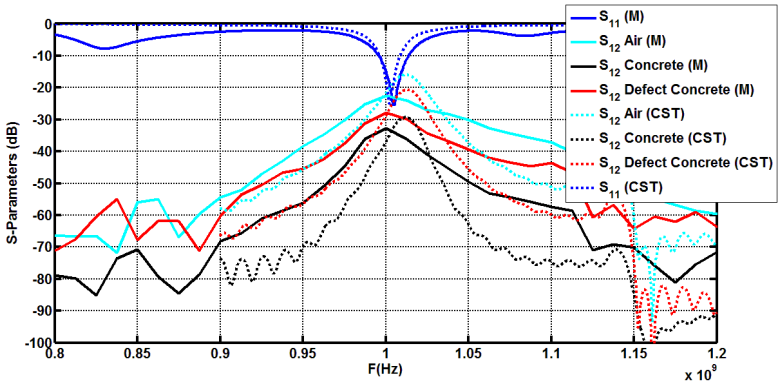

Fig. 23. Measured and simulated S parameters versus frequency of the proposed system.

4. Conclusions

A proposed defected concrete detection system has been introduced. The system consists of two compact antenna arrays with dimensions of 45 cm by 13.2 cm for each and weight of 800 gm for both antenna arrays. The antenna array resonates at 1 GHz and it had a 3 dB beam width of 30.7 degree and directivity of 11.6 dBi which is very suitable for the detection of the defects in a concrete post. The detection principle was relied on the coupling between the antenna array

elements. A 10 dB difference in coupling was obtained between the concrete blocks where the defect was introduced and removed. Proposed measurement system was introduced where the antenna arrays is fixed with a wood stand. The proposed system S parameters are measured using portable VNA for air, concrete and defected concrete block. Good agreement was obtained between measured and simulated one. Finally the proposed system are simple, accurate and low cost relative to its other counterpart systems. The proposed system could be calibrated and used to early detect breast cancer tumors, walls buried objects detection, travellers' bags content and could also be modified to work as a bistatic radar.

References

1. Verma, S.K.; Bhadauria, S.S.; and Akhtar, S. (2013). Review of nondestructive testing methods for condition monitoring of concrete structures. *Journal of Construction Engineering*, 2013, 1-11.
2. Bungey, J.H. (2004). Sub-surface radar testing of concrete, a review. *Construction and Building Materials*, 18(1), 1-8.
3. Zainud-Deen, S.H.; Badr, M.E.; Awadalla, K.H.; and Sharshar, H.A. (2008). Microstrip antenna with defected ground plane structure as a sensor for landmines detection. *Progress in Electromagnetics Research B*, 4, 27-39.
4. Lorenzo, L.M.; Danilo, E.; and Michael, C.W. (2010). Radio frequency tomography for tunnel detection. *IEEE Transactions on Geoscience and Remote Sensing*, 48(3), 1128-1137.
5. Cepni, A.G.; Stancil, D.D.; Henty, B.; Jiang, Y.; Jin, Y.; Moura, J.M.; and Zhu, J.G. (2006). Experimental results on single antenna target detection using time-reversal techniques. *IEEE Antennas and Propagation Society International Symposium*, 703-706.
6. Chen, C.C.; Rao, K.R.; and Lee, R. (2003). A new ultrawide-bandwidth dielectric-rod antenna for ground-penetrating radar applications. *IEEE Transactions on Antennas and Propagation*, 51(3), 371-377.
7. Kim, D.; Cui, X.; Cherala, A.; Chen, K.; and Peroulis, D. (2011). A two-dimensional electronically-steerable array antenna for target detection on ground. *IEEE International Symposium on Antennas and Propagation (APSURSI)*, 734-737.
8. Simi, A.; Manacorda, G.; Miniati, M.; Bracciali, S.; and Buonaccorsi, A. (2010). Underground asset mapping with dual-frequency dual-polarized GPR massive array. *13th International Conference on Ground Penetrating Radar (GPR)*, 1-5.
9. Klemm, M.; Craddock, I.J.; Leendertz, J.A.; Preece, A.; and Benjamin, R. (2009). Radar-based breast cancer detection using a hemispherical antenna array experimental results. *IEEE Transactions on Antennas and Propagation*, 57(6), 1692-1704.
10. Nilavalan, R.; Craddock, I.J.; Preece, A.; Leendertz, J.; and Benjamin, R. (2007). Wideband microstrip patch antenna design for breast cancer tumour detection. *IET Microwaves, Antennas and Propagation*, 1(2), 277-281.
11. Balanis, C.A. (2005). *Antenna theory, analysis and design*. New Jersey: John Wiley and Sons Inc.

12. Stutzman, W.L; and Thiele, G.A. (1998). *Antenna theory and design*. New York : John Wiley and Sons Inc.
13. David, K. (1989). *Field and wave electromagnetic*. New York: Addison Wesley Pub. Co.
14. Kraus, J.D. (1988). *Antennas*. New York: McGraw-Hill.
15. Madhav, B.P.; Sowjanya, J.; Swathi, V.; and Tanmayee, P. (2014). Circular array antenna synthesis based on element spacing. *International Journal of Applied Engineering Research*, 9 (20), 6959-6965.
16. Wong, K. (2004). *Compact and broadband microstrip antennas*. New York : John Wiley and Sons.
17. Ramesh, G. (2001). *Microstrip antenna design handbook*. London: Artech House.
18. Ramesh, G.; Inder, B.; and Maurizio, B. (2013). *Microstrip lines and slotlines*. London: Artech House.
19. Pozar, D.; and Schaubert, D.H. (1995). *Microstrip antennas, the analysis and design of microstrip antennas and arrays*. New York : John Wiley and Sons Inc.
20. Ramkiran, D.S.; Madhav, B.P.; Haritha, N.; Ramya, R.S.; Vindhya, K.M.; and Abhishek, S.P. (2014). Design and analysis of microstrip slot array antenna configuration for bandwidth enhancement. *Leonardo Electronic Journal of Practices and Technologies*, 25, 72-83.
21. Marotkar, M.D.; and Zade, P. (2016). Bandwidth enhancement of microstrip patch antenna using defected ground structure. *IEEE International Conference on Electrical, Electronics, and Optimization Techniques (ICEEOT)*, 1712-1716.
22. Gupta, K.; and Kanaujia, B.K. (2014). Miniturization and bandwidth enhancement of microstrip patch antenna using artificial ground structure. *IEEE International Conference on Industrial and Information Systems (ICIIS)*, 1-4.
23. Lakshmi, S.J.; Khan, H.; and Madhav, B.P. (2015). Design and analysis of high gain array antenna for wireless communication applications. *Leonardo Electronic Journal of Practices and Technologies*, 26, 89-102.